Multiple Representations of Topographic Pattern and Geographic Context Determine Barrier Dune Resistance, Resilience, and the Overlap of Coastal Biogeomorphic Models

Li-Chih Hsu and J. Anthony Stallins

Department of Geography, University of Kentucky

We compared two biogeomorphic models that postulate how vegetation is intertwined in the response and recovery of barrier island dunes. Each model was developed in a separate coastal region using different methods. Both relied on simple elevational representations of topography. By comparing topographies among more islands of these two regions and by linking multiple representations of topographic pattern to resistance and resilience, we provide a synthesis that shows the validity of both models and the consequences of reifying one over the other. Using airborne LiDAR, topographic metrics based on point, patch, and gradient representations of topography were derived for fifty-two sites across eleven islands along the Georgia Bight and Virginia. These seventeen metrics were categorized in terms of resistance and resilience to disturbance from storm-forced high water levels and overwash. *Resistance* refers to intrinsic properties that directly counter expressions of power from disturbance. *Resilience* refers to the degrees of freedom to adjust and adapt to disturbance. Using a cross-scale data modeling approach, these data were visualized as topographic state space using multidimensional scaling. In this state space, similarity in topography as well as resistance and resilience were inferred through a site's position along low-dimension axes representing geomorphic resistance and high-dimension axes representing the spatial landscape properties of biogeomorphic resilience. The two models overlap in how they account for barrier dune resistance and resilience along the U.S. south Atlantic coast. Islands of the Georgia Bight have a propensity for higher resistance and resilience. The Virginia islands have lower resistance and resilience. *Key Words: barrier islands, biogeomorphology, cross-scale structure, dunes, resilience.*

我们比较两个生物地貌模型，该模型假定植被如何在对障蔽岛沙丘之回应与回復中缠绕。两个模型分别在分隔的海岸区域中运用不同的方法建立之。我们通过比较这两个区域中更多的岛屿型态，以及连结多重地形模式再现与抵抗和回復力，提供展现两大模型有效性的合成，以及使其一较另一模型更具体化的结果。运用空中LiDAR，为沿着乔治亚湾和弗吉尼亚的十一座岛屿的五十二个地点，推导出根据点、地块和地形坡度再现的地形度量。这十七个度量，以对于风暴导致的高水位和越流扰动的抵抗及回復力进行分类。抵抗指的是直接反抗扰动力量的展现之固有特质。回復力指的是调整与调适扰动的自由程度。运用跨尺度数据模式化方法，这些数据使用多向度尺度化来可视化成为地形的状态空间。在此状态空间中，通过随着再现地貌抵抗的低向度轴线与再现生物地貌回復力的空间地景属性之高向度轴线的场地位置，推断地形的近似性和抵抗与回覆力 。两个模型在如何解释沿着美国南部亚特兰大海岸的障蔽沙丘的抵抗与回復力上相互重叠。乔治亚湾的岛屿具有较高抵抗与回復力的倾向。弗吉尼亚岛屿则有较低的抵抗与回復力。*关键词：障蔽岛，生物地貌学，跨尺度结构，沙丘，回復力。*

Comparamos dos modelos biogeomórficos que postulan cómo se entrelaza la vegetación en la respuesta y en la recuperación en una barrera de dunas insulares. Cada modelo se desarrolló en una región costera separada usando métodos diferentes. Ambos dependieron de simples representaciones de altura de la topografía. Al comparar las topografías entre más islas de estas dos regiones, y conectando múltiples representaciones del patrón topográfico a la resistencia y la resiliencia, generamos una síntesis que muestra la validez de los dos modelos y las consecuencias de reificar a uno sobre el otro. Usando el LiDAR aéreo, métricas topográficas basadas en punto, parches y gradiente, se derivaron representaciones de la topografía para cincuenta y dos sitios a través de once islas situadas a lo largo de la Bahía de Georgia y Virginia. Estas diecisiete métricas se categorizaron en términos de resistencia y resiliencia a la perturbación por niveles altos de agua forzados por la tormenta y por overwash. La resistencia se refiere a las propiedades intrínsecas que directamente enfrentan

Annals of the American Association of Geographers, 0(0) 2019, pp. 1–21 © 2019 by American Association of Geographers
Initial submission, January 2019; revised submission, May 2019; final acceptance, June 2019
Color versions of one or more figures in the article can be found online at www.tandfonline.com/raag
Published by Taylor & Francis, LLC.

las expresiones de poder de la perturbación. La resiliencia se refiere a los grados de libertad de ajustarse y adaptarse a la perturbación. Usando un enfoque de modelado de datos de escala cruzada, los datos se visualizaron como espacio en estado topográfico usando procedimientos de escala multidimensional. En este espacio estado, la similitud en topografía lo mismo que la resistencia y la resiliencia se dedujeron a partir de una posición del sitio a lo largo de ejes de dimensiones bajas que representan la resistencia geomórfica, y de ejes de dimensiones altas que representan las propiedades del paisaje espacial de la resiliencia biogeomórfica. Los dos modelos se traslapan en lo que concierne a cómo considerar la resistencia de la barrera de dunas y la resiliencia a lo largo de la costa sudatlántica de los EE.UU. Las islas de la Bahía de Georgia tienen una propensión a resistencia y resiliencia más altas. Las islas de Virginia tienen resistencia y resiliencia más bajas.
Palabras clave: barrera insular, biogeomorfología, estructura de escala cruzada, dunas, resiliencia.

Spatial pattern comparison is a fundamental mode of geographic inquiry, one that has taken on urgency in light of accelerating anthropogenic environmental change. For physical geographers, spatial pattern comparison is augmented by the increased availability of data collected at high resolution and large spatial extents. These data have made it possible to compare the spatial attributes of landforms in new and more subtle ways (Long and Robertson 2017; Praskievicz 2018). This is particularly true for sandy barrier island coasts, where higher sea levels and more frequent storm surges are anticipated if not well underway.

Although questions about the processes and patterns contributing to the maintenance of barrier islands motivated scholars in the 1970s and 1980s (Godfrey 1977; Godfrey, Leatherman, and Zaremba 1979; Leatherman 1979), their focus now is more attentive to the extent to which these landforms will exhibit resilience to human-caused climate change (Moore and Murray 2018). Resilience has two properties. *Engineering resilience*, or *resistance*, refers to properties that directly counter expressions of power from externally forced disturbances like storm surge. *Ecological resilience*, herein *resilience*, is a measure of the degrees of freedom a system has evolved to absorb or adjust to disturbance before changing state. This dual, or bivariate, aspect of resilience is recognized by biogeographers and geomorphologists (Stallins, Mast, and Parker 2015; Phillips and Van Dyke 2016; Thoms, Metizen et al. 2018; Thoms, Piégay, and Parsons 2018; Fuller et al. 2019).

In these renewed inquiries about the forces that maintain barrier islands, dune topography is recognized as a critical determinant of how sandy coasts respond to and recover from high water events. One ongoing line of investigation emphasizes process-based geomorphic and geologic mechanisms. Sediment exchange among dunes, the nearshore, and the beach controls dune height. In turn, dune height shapes the overland transfer of sediment and the maintenance of barrier island elevation (Houser 2018). Geological framework, bathymetric features, dune topographic variability, and storm sequence are interwoven factors shaping sediment exchange (Houser 2013; Houser et al. 2015; Hapke et al. 2016; Walker et al. 2017; Wernette, Houser, et al. 2018). The emphasis in these reductionist barrier island studies (*sensu* Harrison 2001) is on elucidating the geomorphic variables and conditions that maintain barrier islands, often for the development of predictive models (Gutierrez et al. 2015; Houser, Wernette, and Weymer 2018; Weymer et al. 2018).

An accompanying line of inquiry into the forces that maintain barrier islands emphasizes the emergent properties of dune topography (Stallins 2005; Wolner et al. 2013; Brantley et al. 2014; Vinent and Moore 2015; Zinnert, Shiflett, et al. 2016). These studies also aim to describe the response and recovery behavior of barrier dunes when exposed to high water events. They concentrate on the potential contributions of ecological and biogeomorphic phenomena, however. The overland transfer of sediment is also shaped by feedbacks among dune topography, dune vegetation, and meteorological forcings that elevate water levels and mobilize sediments. The dune dynamical states of Vinent and Moore (2015) and Goldstein and Moore (2016) document how barrier dunes along the Virginia coast can become trapped in a low topographic state or maintain elevation through dune building as a high topographic state. Whether topography on Virginia barrier islands can recover from a low, frequently inundated state is determined by the balance of constraints imposed by sediment availability, the stabilizing effects of vegetation, plant growth rates, and the timing of storm sequences. In the stability domain

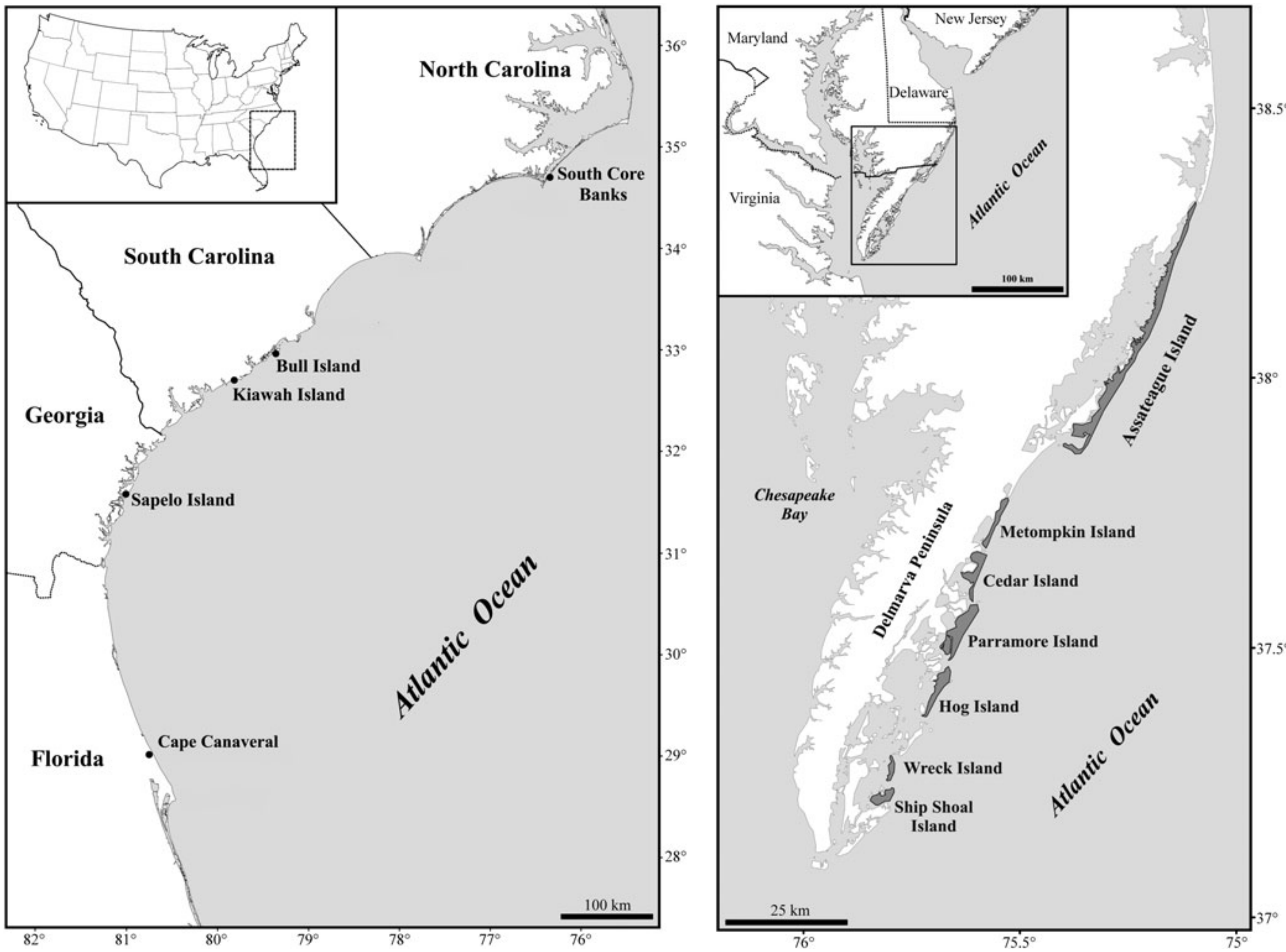

Figure 1. Study islands in the Georgia Bight and along the Virginia coast.

model of Stallins and Parker (2003), similar high and low island states are defined in terms of plant functional types and how they shape the spatial attributes of the dune landscape. In a disturbance-reinforcing stability domain, frequent overwash forcing events and biogeomorphic feedbacks reinforce a resilient assemblage of dune plant functional types. These plants lower topographic resistance to overwash, as postulated for the wave-dominated barrier island morphology of South Core Banks, North Carolina. In a disturbance-resisting stability domain, infrequent overwash forcing events and biogeomorphic feedbacks reinforce a resilient assemblage of dune plant functional types that augments topographic roughness and increases resistance to overwash, as postulated for the tidally dominated barrier island morphology of Sapelo Island, Georgia. The high and low state model and the stability domain model do not necessarily apply to an entire island but to coastal stretches within an individual island (Zinnert, Brantley, and Young 2016).

These two biogeomorphic models each seek to understand the resilience properties of barrier coasts. The high and low state model places an emphasis on the net balance among geomorphic and biogeomorphic processes that maintain an island, however. The stability domain model stresses the landscape spatial character of biogeomorphic interactions. In addition, the Virginia high and low state model is derived from modeling and remote sensing. The Georgia Bight stability domain model is based on ground-based sampling of topography and vegetation. Yet both models are generalized from a few islands. The characterizations of topography that inform each of them are based only on simple point and line elevations. Taken together, these two models reflect a tension between simplifications of topography done as a prerequisite for modeling versus those made in field investigations trying to incorporate geographical verisimilitude (Vinent and Moore 2013; Davidson-Arnott et al. 2018).

To identify the common ground between these two models, we compared dune topographies across six barrier islands of the Georgia Bight to topographies among seven islands of the Virginia barrier coast (Figure 1). We posed two questions: (1) How do the dune topographies of the Georgia Bight and Virginia coastal region differ? (2) How do the dunes in these regions differ in resistance and resilience? The barrier islands of the Georgia Bight are composed of tidally dominated island morphologies toward its center and wave-dominated island morphologies along its limbs in Florida and North Carolina. Along these two outlying coastlines, tidal range is at a minimum and wave heights are high. Barrier island morphologies tend to be long and narrow. Toward the center of the bight, where tidal range increases and wave heights diminish, barrier islands tend to be shorter and wider. Hayes (1994) classified the Georgia Bight islands into the wave-dominated barrier islands of the Outer Banks of North Carolina, the mixed tidal and wave energy barrier islands of South Carolina, the tide-dominated estuarine sea islands of Georgia, and the wave-dominated barrier islands along the east coast of Florida.

The Virginia barrier islands are a part of the Delmarva Peninsula. Headland erosion at the northern extent of the peninsula provides sediments for Assateague Island, a wave-dominated barrier island, and for the more numerous mixed-energy, tide-dominated barrier islands to the south (Oertel and Kraft 1994). Rates of relative sea level rise from New Jersey to North Carolina are among the highest along the U.S. Atlantic coast (Sallenger, Doran, and Howd 2012; Piecuch et al. 2018). Many of the Virginia islands are migrating toward the mainland and are undergoing pronounced reductions in upland area (Zinnert, Shiflett, et al. 2016; Deaton, Hein, and Kirwan 2017).

By comparing topographic patterns in these two regions, our intent was to infer the consequences of the simplifications and generalization inherent to the existing biogeomorphic models. The topographic variables informing these models have been limited to primary foredune height or field-observed point elevations along line transects even though alongshore topographic variability (Houser, Wernette, and Weymer 2018) and spatial biogeomorphic processes (Feagin et al. 2005) are important. By incorporating a greater variety of ways to represent topography in these comparisons, we provide a more nuanced assessment of where and under what conditions different levels of barrier dune resistance and resilience develop. In these comparisons, it was not feasible to incorporate all of the geologic, bathymetric, and meteorological factors that impinge on barrier island dune topography. Dune topography, however, is the proximate causal factor influencing the movement of sediment and the maintenance of a barrier island. Furthermore, as a strategy of geographers, comparisons among many different places generate knowledge in ways that fully specified descriptions of one or a few locations do not. From the perspective of macroecology (McGill [2019] and many others), the relationships between topography and resilience properties can be more readily discerned by comparing observations from many islands.

Resistance, Resilience, and Comparing Spatial Patterns

We employ the definition of resilience that recognizes its multiple components. Geomorphologists and ecologists describe resilience as bivariate (Thoms, Piégay, and Parsons 2018; Fuller et al. 2019) in that there are two interrelated properties of resilience. Engineering resilience, or resistance, refers to properties that directly counter expressions of power from extrinsic disturbance. Ecological resilience (i.e., resilience) is a measure of the degrees of freedom that have evolved to absorb or adjust to disturbance. Resilience is a measure of how feedbacks couple to extrinsic disturbance and maintain an organizational structure and function until some threshold is reached and the system undergoes a change in state. Resistance is a measure of the magnitude of change as an immediate response to disturbance. Resilience invokes adaptation and the emergence of stabilizing feedbacks.

Biophysical systems can have varying levels of resilience properties simultaneously (Corenblit et al. 2009; Corenblit et al. 2015; Eichel, Corenblit, and Dikau 2016; Hortobágyi et al. 2018). Resilience emerges out of resistance and they shape one another. Plant adaptations and biogeomorphic feedbacks might enhance resistance to disturbance if disturbance-forcing events are frequent. Conversely, plant adaptations and biogeomorphic feedbacks could lessen resistance where disturbance-forcing events are infrequent. By modulating disturbance exposure, biogeomorphic interactions can select for resilient configurations of landforms, sediment mobilities, and plant compositions. Extreme resistance to disturbance or minimal resistance might inhibit the development of landform–vegetation feedbacks that contribute to the emergence of resilience.

Inferring resistance and resilience among different topographies requires addressing the underacknowledged intricacy of making spatial pattern comparisons (Lastochkin, Zhirov, and Boltramovich 2018; Praskievicz 2018). A single pattern can have a variety of components and be represented in various ways. As Wernette, Thompson, et al. (2018) noted, many studies have made predictions about dune change based on a few summary measures of topography. Topography has often been limited to point observations averaged for an area on an island or calculated within a moving window distance. Topography is also frequently represented as a line demarcating the alongshore elevation of the primary foredune crest or the beach berm. If sandy barrier islands are composed of spatially interactive landscape elements as postulated (Odum, Smith, and Dolan 1987; Feagin et al. 2005; Feagin and Wu 2007), elevation and topography should be characterized in multiple ways. Elevations can also be represented as an area bounded by contour lines. As in a classed choropleth map, elevation point observations can be reclassified into discrete intervals to form polygons or patches of different sizes and shapes. Elevation also has properties arising from its continuous distribution as a spatially explicit gradient representation (Kedron et al. 2018). Singular measures of elevation might be useful, but they are also incomplete descriptions of spatial pattern. By using multiple representations of topography like these, one can extract more information and make more nuanced pattern comparisons. This also allows different conceptual paradigms to contribute to pattern-process interpretations. The choice of paradigm can influence the outcomes of inquiry. Conclusions about ecological and geomorphic phenomena can differ based on whether a patch or a gradient paradigm was employed (van Coller, Rogers, and Heritage 2000; Stallins 2006; Collins et al. 2018). Combining multiple representations of dune topography is also strategic because of the uncertainties inherent to reliance on a few measures of elevation (Wernette, Thompson, et al. 2018).

Yet even if multiple representations of topographic pattern improve comparisons, what still remains a challenge is ensuring that pattern reflects process. For them to remain linked, a larger theoretical framework is needed to guide what data representations are selected and how they can be combined prior to making comparisons (Praskievicz 2018). In this study, the ecological concept of cross-scale resilience provided the framework to ensure that pattern and process were linked. Cross-scale resilience postulates how variability in pattern and process within and across scales confers resistance and resilience (Nash et al. 2014; Allen et al. 2016). Its origins borrow from hierarchy theory, but cross-scale resilience accounts for more of the adaptive and evolving nature of biophysical systems. Cross-scale resilience is not just a conceptual description. Many authors use the term *cross-scale resilience* to acknowledge that interactions promoting resilience occur across scales. The concept of cross-scale resilience comes with empirics (Allen et al. 2016; Sundstrom et al. 2018). Cross-scale resilience provides a theory-based methodology to account for resilience properties generated through the structural relationships among a few key driving variables.

Operationalizing Cross-Scale Resilience to Compare Dune Topography

Cross-scale resilience properties have been quantified in terrestrial, marine, and socioecological systems (Nash et al. 2014; Sundstrom et al. 2014; Sundstrom et al. 2018). Modeling cross-scale resilience begins with the specification of variables, or metrics, that represent compartmentalized but nested cycles of pattern and process. In resilience theory, these are known as adaptive cycles. When linked across local to landscape extents, these cycles summarize successional development (Allen et al. 2014; Hortobágyi 2018). This linked structure is known as a *panarchy*. The metrics that specify the individual cycles of development in a panarchy should target the key structuring processes occurring at different scalar extents (e.g., Walker et al. 2017), thereby entailing the use of different representations of pattern. Based on Stallins and Corenblit (2018), what follows is an explanation of how the metrics selected in our cross-scale model correspond to resistance or resilience, what facet of dune topography they represent, and how these metrics can be integrated to compare dune topographies and link them to resilience properties.

The geomorphic processes that determine elevation comprise the lowest compartment in our cross-scale data model. For a given location, elevation encompasses cycles of sediment deposition and erosion derived through wind and wave energy as well as sediment availability. Elevation is a foundational resistance metric. It plays a large role in how high-water events affect topography. The next compartmentalized cycle of our data model spans the additional resistance conferred by the anchoring effects of vegetation and the development of dune landforms of different size and shape. Resistance here varies with cycles of dune plant population expansion and destruction associated with geomorphic disturbances like blowouts and overwash. Low levels of resilience can emerge through the processes summarized in this second compartment, because the size and shape of individual dune landforms and dune plant abundances could reinforce each other in a positive feedback under the prevailing geomorphic disturbance regime. These dune landforms can be represented by metrics expressing the different sizes and shapes of polygons or patches formed by classification of elevational intervals.

Resilience is potentially at a maximum in the next highest compartment. Biogeomorphic processes, ecological interactions, and topography can become spatially integrated and reinforce one another through positive feedbacks encoded across the landscape as a form of ecological memory. This resilience can be represented by metrics that capture the continuous surface features of topography. These gradient metrics reflect how topography can shape the connectivity or resistivity to flows of sediments, storm surge, and plant propagules. In dunes, interactions at one point on the landscape can influence conditions at another (Reiners and Driese 2001; Feagin et al. 2005; Feagin and Wu 2007).

Topographic comparisons can then be made by assessing the variance structure of these data. Because the metrics of a cross-scale data model are hierarchically nested, they will have multicollinearity. Through dimensionality reduction techniques like ordination, the variance comprising this multicollinearity can be partitioned across different dimensions, typically orthogonal axes. As visualized in a scatterplot, the position of island sites in this space reflects their topographic differences. Each axis can then be affiliated with trends in resistance or resilience based on which topographic metrics load more strongly on them (Lamothe, Somers, and Jackson 2019). In this topographic state space, topography and resilience properties can be compared simultaneously. Geomorphologists have employed analogous approaches, like morphospace, phase space, or evolution space (Inkpen and Petley 2001; Phillips 2009; Baas and Nield 2010; Inkpen and Hall 2016; Phillips 2018b). Any single landscape should be capable of being located within a larger state space derived from multiple landscapes or else expand the boundaries of this state space if it has not been encountered before.

For a state space constructed in this manner, the number of axes (i.e., its dimensionality) summarizes the nonindependent relationship between resistance and resilience. Following Donohue et al. (2013), Hillebrand et al. (2018), and Radchuk et al. (2019), resilience is a higher dimensional property that emerges out of the resistance that develops at lower dimensions. As expressed in terms for barrier island dunes, lower dimensional axes of state space summarize trends in geomorphic resistance. Higher dimensional axes summarize trends in resilience. This resilience arises through biogeomorphic and ecological processes that modify the geomorphic template and shape landscape spatial structure. Thus, the number of axes as well as how individual variables load on these axes becomes the basis for comparing topography and for inferring how resistance and resilience covaries with topography.

Methods

Study Area and Sampling Design

Dune topography in the Georgia Bight was characterized on five islands: Cape Canaveral (Florida), Sapelo Island (Georgia), Bull Island (South Carolina), Kiawah Island (South Carolina), and South Core Banks (North Carolina). Dune topography was characterized for seven islands along the Virginia and Maryland coasts, from north to south, Assateauge Island, Metompkin Island, Cedar Island, Hog Island, Parramore Island, Wreck Island, and Ship Shoal Island.

The general locations to sample topography along the shore of each island were first visually identified in Google Earth imagery. The time frame was limited to the most recent years for which LiDAR data were available that spanned multiple islands. This visual method encompassed identification of the topographically distinctive, contiguous coastal strands along an island. It was analogous to how the fluvial unit of the river reach guides field sampling in fluvial settings. Criteria to detect the predominant topographies within an island included beach width, the width of the dune field, linearity of the dunes, and type of habitat behind dunes. Areas of pervasive human impact and locations directly on tidal inlets were excluded. Three to five distinctive stretches of topography were adequate to capture the range of topographies on each island. A square plot was randomly located within each distinctive reach of barrier island dune shoreline. Study plots initiated at the mean high-water mark datum (MHW) and extended inland to where salt marsh or dense stabilized woody vegetation developed. Fifty-two sites from twelve islands were sampled.

LiDAR Data

Digital elevation models (DEMs) were constructed for sites along each island using LiDAR ground elevations obtained online from the National Oceanic and Atmospheric Administration's (NOAA's) Coastal Services Center. Dune topographic metrics for the Georgia Bight utilized a 2010 LiDAR data set collected by the U.S. Army Corps of Engineers for four of five islands. Vertical (horizontal) accuracy was 15 cm (75 cm) and nominal point space was 2 m. Due to small gaps in this 2010 data set, topographic metrics for South Core Banks were constructed from post-Sandy LiDAR data sets collected by the U.S. Geological Survey in 2012. For these data, vertical (horizontal) accuracy was 7.5 cm (19.4 cm) and nominal point space was 1 m. A post-Hurricane Sandy data set (2014) collected by the NOAA National Geodetic Survey was used to construct DEMs for sites on the Virginia islands. Vertical (horizontal) accuracy was 6.2 cm (100 cm) and nominal point space was 0.3 m. To assess the sampling design, Parramore Island was sampled twice, independently, first with the 2012 LiDAR data set in Monge and Stallins (2016) and a second time as part of the Virginia sampling with the 2014 LiDAR data set.

LiDAR point elevations were resampled to a resolution of 1 m and then interpolated using inverse distance weighing to fill any gaps. LiDAR processing was performed in ArcGIS using LAStools (Isenburg 2014). The Virginia MHW shoreline was defined as the 0.7 m contour line relative to the NAVD 88 datum following Rogers et al. (2015). The islands in the Georgia Bight and the replicate plots for sites on Parramore were referenced to the MHW mark using VDatum (NOAA 2012).

Topographic Metrics

The broad-extent, high-resolution coverage of LiDAR point data aids in the derivation of multiple representations of topography (Fonstad and Marcus 2010; Long and Robertson 2017). Three sets of topographic metrics were produced, one for each compartment. LiDAR point observations were (1) analyzed at the site level to derive elevational descriptive statistics (resistance metrics); (2) categorized into intervals within sites to produce indexes of landform patch structure (resistance and resilience metrics); and (3) summarized across the continuous surface of a site as a gradient representation (resilience metrics).

The first set of metrics, elevational descriptive statistics, included mean, maximum, median, 25th percentile, and 75th percentile elevations derived from the 1-m point observations of each site DEM. These low-dimension metrics target geomorphic resistance, the susceptibility to exposure to maritime inputs. The second set of metrics consisted of indexes produced from FRAGSTATS software (McGarigal, Cushman, and Ene 2012). These metrics capture resistance as well as any nascent biogeomorphic resilience expressed in the size and shape of individual dune landforms. Landforms' size and shape influence response and recovery to high-water events. To derive the patches demarcating dune landforms, raster DEMs were converted into areal representations following Wu et al. (2017) and Ryu and Sherman (2014). The number of elevation classes was reclassified from all possible centimeter intervals in the LiDAR point observations to one based approximately on decimeter intervals. A patch is the areal form taken by these decimeter elevation intervals.

Eight FRAGSTATS indexes were deemed well suited for discerning dune pattern–process relationships following Kupfer (2012). The aggregation index (AI) increases with greater patch coalescence and size. The area-weighted mean shape index (SHAPE_AM) increases as patches become more curvilinear. Higher values for the interspersion and juxtaposition index (IJI) indicate that patches are equally adjacent to all other patches. Higher values for the largest patch index (LPI) imply a greater dominance of a single patch type. A higher Simpson's diversity index (SIDI) implies higher patch richness and more equitable patch abundance. For the perimeter-area fractal dimension index (PAFRAC), all patch shapes tend to be convoluted when this value is large. The contagion index (CONTAG) increases as patches become larger and dominated by a single elevational range. The landscape shape index (LSI) increases as intervals of elevation become less clumped and more aggregated. Erosional, low-relief barrier dunes would be expected to have a high aggregation (AI), more pronounced curvilinear and convoluted landforms (SHAPE_AM, PAFRAC), and the dominance of one or few patch type and decimeter elevational ranges (LSI, LPI, CONTAG). Patch diversity (SIDI) and the intermixing of patches (IJI) would be expected to decline. Conversely, barrier dunes with less erosion would be expected to have less patch aggregation, more rectilinear patch forms, and less dominance of a single patch elevational range. Patch diversity and the intermixing of patches would be expected to increase.

The third set of metrics summarizes resilience encoded in the continuous, gradient spatial structure of the landscape. They reflect the connectivity among different biogeomorphic components of the landscape. They included the skewness and kurtosis of point elevation values, the spatial autocorrelation structure of elevation, and plot size. Skewness, kurtosis, and spatial autocorrelation are properties associated with critical transitions in resilience (Scheffer et al. 2015). Skewness and kurtosis were derived from all point observations across a site DEM. Spatial autocorrelation was summarized in directional correlograms derived from the 1-m DEM surface in GS$^+$ software (Robertson 2008). These were constrained to directions perpendicular to the water line. Autocorrelation was assessed up to the distance lag representing the width of the plot. Six Moran's *I* values from the major breaks along the plot of Moran's *I* were taken from each correlogram and ordinated with principal coordinates analysis (PCoA) to convert correlogram structure into values that could be ordinated with the other dune topographic metrics. All PCoA ordinations reduced down to one significant axis, and the *x* coordinate for this axis was used as the autocorrelation metric. The size of the plots, expressed as the length of an edge of a site DEM in meters, was included as a metric because this parameter is the constraint within which any topographic pattern and its resilience properties are confined.

Constructing State Space

The cross-scale topographic metrics for the Georgia Bight region and the Virginia coast data sets were ordinated using nonmetric multidimensional scaling (NMDS) separately and then as a combined data set. The NMDS algorithm first calculated a similarity distance matrix based on the seventeen metrics of dune topography characterized for each island site. The next step in NMDS was to fit these similarity distances into a low (typically two- or three-) dimensional state space. This required iteratively shuffling the positions of sites in this state space until an optimal solution was found, one that preserved the similarities in the original distance matrix while minimizing the number of dimensions, or axes. Stress is a measure of how well matrix similarity distances correspond with their graphical solution. NMDS solutions can be assessed for significance by comparing reduction in stress in the actual data with reduction observed with randomizations of these data. All topographic metrics were relativized as *z* scores prior to ordination. Similarity distances were Euclidean. The final solution was subjected to an orthogonal rotation to maximize variance in the data set along the first and succeeding axes. Pearson's correlation coefficients were derived from the coordinates of island sites along each NMDS axis and the standardized values for the topographic metrics. Hierarchical cluster analysis of the final combined data set was performed using a flexible beta group linkage method ($\beta = -0.25$). Ordinations and clustering were performed in PC-Ord Version 7 (McCune and Mefford 2016).

Hypotheses

The islands from the Georgia Bight were expected to have more varied topography because of this region's greater contrasts in nearshore conditions and barrier

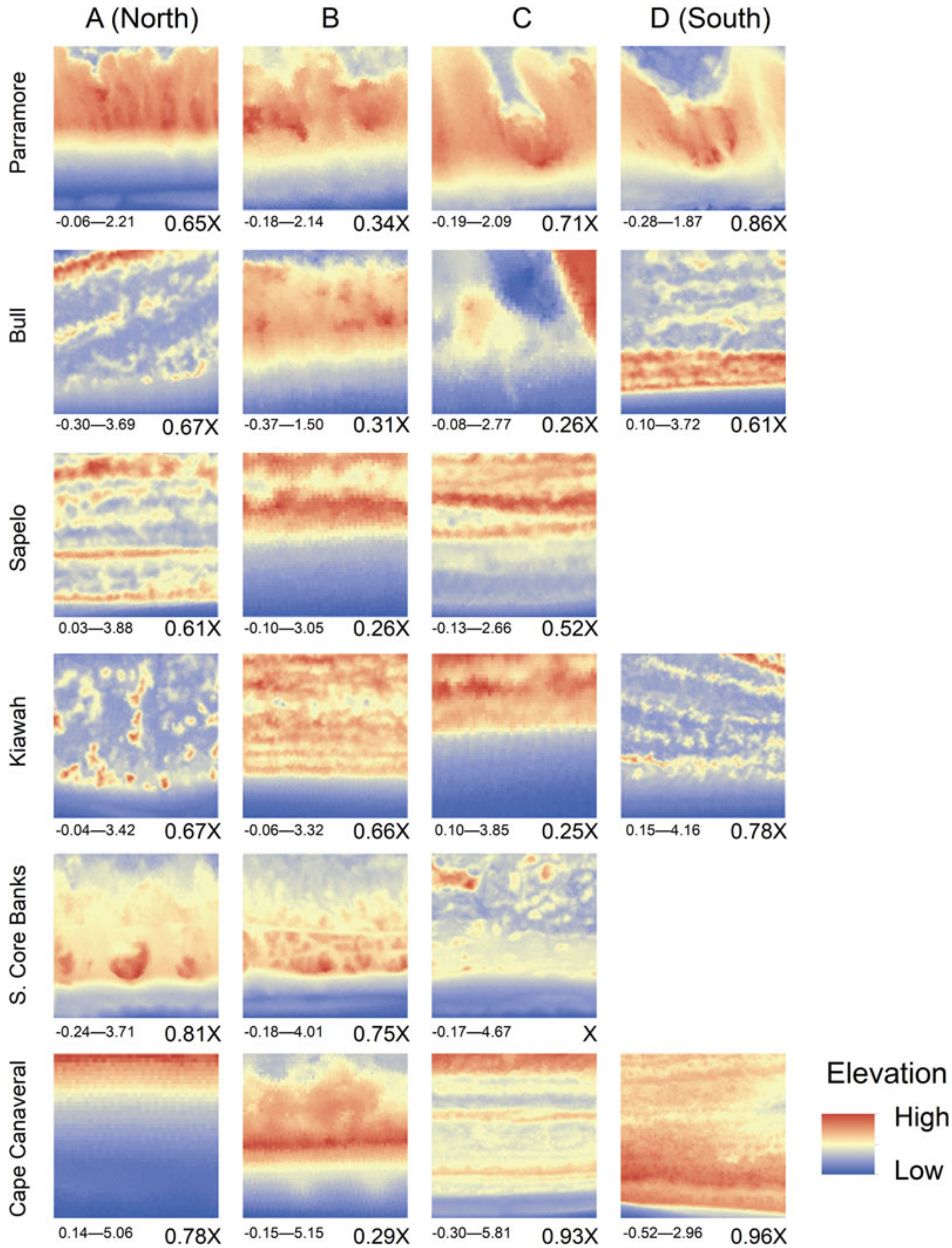

Figure 2. DEMs for study sites along the Georgia Bight, scaled to local minimum and maximum elevations. Letters indicate position along the island from A (northernmost) to D (southernmost). Site DEMs differed in size, although they are scaled to be the same here. The conversion factors below each DEM can be used to derive their size relative to the largest site, South Core Banks C (215 m × 215 m). For example, the observed dimensions of site C on Sapelo Island are 112 m × 112 m (0.52 × 215 m = 111.8 m). DEM = digital elevation model.

island morphology. The islands sampled in the Georgia Bight are also not as consistently low and erosional as those in Virginia. Consequently, we expected that the state space solution for the Georgia Bight would have a higher dimensionality. Dune elevation statistics, patch indexes, and gradient metrics should separate out along multiple axes and exhibit less multicollinearity because of the potentially stronger influence of dune vegetation on the secondary modification of topography. Because the Virginia barrier islands are experiencing rapid rates of retreat and sea-level rise, we expected their dimensionality to be lower. With

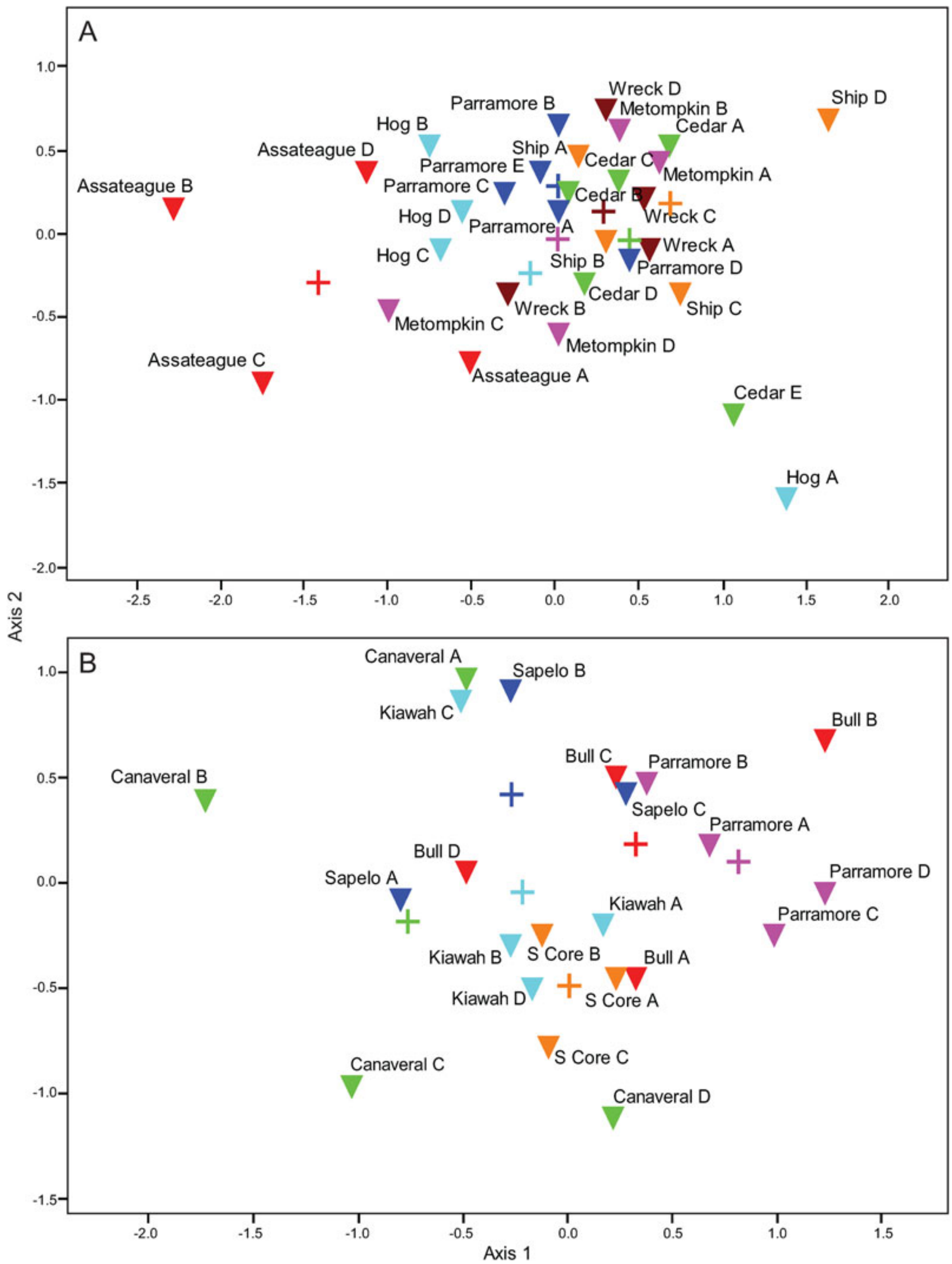

Figure 3. Nonmetric multidimensional scaling topographic state space for (A) the Georgia Bight and (B) the Virginia coast. Symbol colors indicate island membership.

more frequent high-water events, higher dimension spatial metrics for patch and gradient representations should have greater collinearity with elevation.

Lower resistance and resilience were expected for the Virginia islands because the patterns of topography should be more directly coupled to frequent storms and the low, erosional status of the islands. On islands in the Georgia Bight, resistance and resilience were expected to be greater. The secondary modification of topography through biogeomorphic processes should be less affiliated with erosion, thereby facilitating the development of positive feedbacks among landforms, vegetation, and overwash disturbance regime associated with high

Table 1. Dimensionality, stress, and variance extracted for state space axes

	Axis 1	Axis 2	Axis 3	Final stress or total variance extracted
Virginia state space ($n = 30$ plots)				
Stress	42.0	13.7		11.5
Variance	43.7	22.2		65.8
Georgia Bight state space ($n = 22$ plots)				
Stress	45.6	15.5	5.1	4.5
Variance	40.6	27.9	15.0	83.5
Combined state space ($n = 52$ plots)				
Stress	41.8	12.8		11.1
Variance	48.6	20.7		69.3

Notes: All values significant ($p < 0.01$) based on Monte Carlo permutations of the observed data. Variance derived from principal coordinates analysis.

resilience. All of these hypotheses were expected to be reflected in the position of island sites relative to the low- and high-dimensional axes of state space.

Results

Georgia Bight Topographic State Space

Topographies in the Georgia Bight (Figure 2) varied from shore-parallel, rectilinear dune ridges and swales (Kiawah B, Sapelo A, Canaveral D) to patchy, overwash topographies (Kiawah A, South Core Banks C, Bull A). The optimal NMDS solution for the Georgia Bight required three dimensions (Figure 3A). Stress on all three axes was lower than randomizations (Table 1). Dune topography differed within individual islands to the extent that many site topographies had greater similarity to sites on other islands. For example, Sapelo C was more similar to Parramore B than to other Sapelo sites. Pearson's correlations for the first NMDS axis were strongest for elevational statistics, patch aggregation, patch shape, and patch diversity (Table 2). Thus, to the left in state space along the first axis, elevations became higher and less aggregated and exhibited variability over relatively small distances. Dunes were more rectilinear in shape. Toward the right along the first axis, site elevation decreased and exhibited less variability over wider areas. Elevation patches became more aggregated and curvilinear in shape. For the second axis, stronger correlations developed for patch interspersion, the landscape shape index, spatial autocorrelation, and plot size. Thus, island plots toward the top of state space are areally small and no one decimeter elevational interval was dominant. Spatial autocorrelation of elevation remained near zero at increasing distance lags because of their more variable topography. Sites toward the bottom of state space were larger in size and patches had little elevational variability. The spatial autocorrelation of elevation became increasingly negative at greater distance lags. The third axis exhibited a robust correlation only with skewness.

Virginia Dune Topographic State Space

The DEMs for Virginia exhibited patchy, fragmented topographies (Assateague B, Wrecks A and B, Cedar D, Ship Shoal C) as well as broad areas of low, flat topographies (Cedar A, Metompkin B, and Wreck D; Figure 4). Shore-parallel rectilinear ridges were weakly expressed and tended to occur as a single feature in the middle or rear of a site (Metompkin C, Hogs A and C). The optimal NMDS solution required two dimensions (Figure 3B; Table 1). Axis correlations were weaker (Table 3). Robust correlations for the first axis included only elevational statistics, patch aggregation, and patch diversity. Topographies along the second axis varied according to changes in plot size and in the skewness and kurtosis of elevation. To the left (right) of state space along the first axis, sites become higher (lower) and patch elevations are more (less) diverse and less (more) aggregated. To the top (bottom) of the scatterplot, plots become smaller (larger), more negatively (positively) skewed, and more negatively (positively) kurtotic. Dune habitats on Wreck D and Parramore B, for example, are smaller and have a long tail of elevations in the direction of a few low elevations. On Hog A and Cedar E, the distribution of elevations is strongly peaked around low elevations with a long tail of observations in the direction of a few higher elevations.

Table 2. Pearson's correlation coefficients for plot nonmetric multidimensional scaling axis coordinates and topographic metrics for the Georgia Bight

	Axis 1	Axis 2	Axis 3
Descriptive statistics (resistance)			
Mean elevation	**−0.89**	−0.26	−0.29
Max elevation	−0.56	−0.22	0.19
25th percentile elevation	**−0.71**	−0.62	−0.23
50th percentile elevation	**−0.80**	−0.33	−0.45
75th percentile elevation	**−0.88**	−0.02	−0.37
Patch metrics (resistance and resilience)			
Aggregation index	**0.89**	−0.17	−0.35
Contagion	0.59	−0.66	0.05
Interjuxtaposition	−0.56	**0.74**	0.11
Large patch index	0.57	0.52	0.05
Landscape shape index	−0.33	**−0.87**	0.15
Perimeter-area fractal dimension	−0.60	−0.14	0.31
Mean shape index	**0.78**	−0.39	−0.34
Patch diversity	**−0.80**	0.27	−0.30
Gradient surface metrics (resilience)			
Skewness of point elevations	−0.12	0.16	**0.87**
Kurtosis of point elevations	−0.03	−0.66	0.68
Directional spatial autocorrelation of elevation	−0.17	**−0.75**	0.59
Plot size	0.17	**−0.93**	−0.13

Notes: Correlations deemed important were >0.70 and not influenced by outliers (shown in bold).

Combined Topographic State Space

A two-dimensional NMDS solution was optimal (Table 1). Sites as well as island centroids indicated that the Georgia Bight and Virginia topographies occupied distinct regions in state space (Figure 5A). With hierarchical clustering into two groups (Figure 5B), only one site from the Georgia Bight (Bull B) fell within the cluster for the Virginia barrier islands. Virginia sites from Metompkin, Hog, Assateague, and Wreck clustered with the Georgia Bight data. The site topographies for Parramore Island sampled independently plotted close to one another, signifying that the sampling design was not unduly biased. Clustering at the level of seven groups (Figure 5C) differentiated dune topographies along the second axis. The variability in topography expressed along the second axis was contained mostly within islands in the Georgia Bight.

The first axis of combined state space was structured by trends in elevation and FRAGSTATS indexes (Table 4). Elevations became lower and topographic homogeneity increased to the right of state space. To the left, elevations were higher and more variable over smaller distances and dune landforms became more rectilinear. The second axis correlations were higher for kurtosis, the landscape shape index, and plot size. Toward the top (bottom) of the combined state space, the size of the dune habitat became smaller (larger), patches of elevation were less (more) dominated by a few elevation intervals, and elevations had a less (more) peaked distribution of elevations.

Discussion

The concept of disturbance-resisting and disturbance-reinforcing barrier island stability domains and attributions of their resilience properties originated from a small set of field observations on two greatly contrasting island morphologies, the tidally dominated island of Sapelo Island, Georgia, and the wave-dominated island of South Core Banks, North Carolina (Stallins 2005). The stability domain idea was then extended to the Virginia barrier islands (Wolner et al. 2013; Brantley et al. 2014; Zinnert, Stallins, et al. 2016). The Virginia islands became the setting for the development of the high and low island state model of Vinent and Moore (2015). The modeling and remotely sensed field verifications that inform the Virginia model were derived from dune elevations, a singular but important determinant of the outcome of exposure to high water levels (e.g., Sallenger 2000). By contrast, the more descriptive,

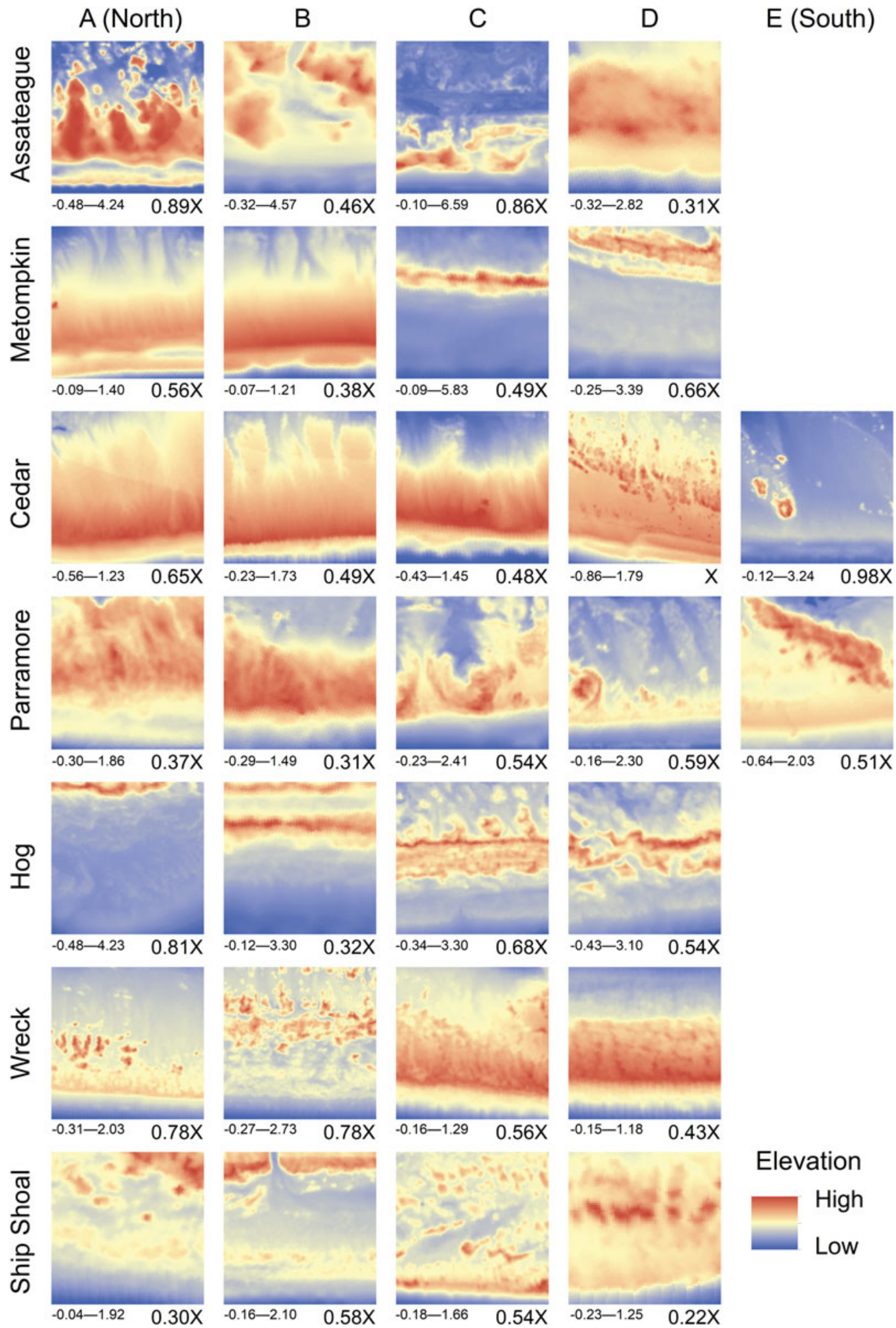

Figure 4. Digital elevation models of Virginia study plots, scaled to local minimum and maximum elevations. See Figure 2 for explanation. The largest island site is Cedar D (295 m × 295 m).

field-based stability domain model places more emphasis on the landscape interactions of landforms and dune plant functional abundances affiliated with the two prominent classes of barrier island morphology. Although each model relies on different representations of topography, this is likely a function of

Table 3. Pearson's correlation coefficients for plot of nonmetric multidimensional scaling axis coordinates and topographic metrics for Virginia barrier islands

	Axis 1	Axis 2
Descriptive statistics (resistance)		
Mean elevation	**−0.91**	−0.24
Max elevation	−0.64	−0.65
25th percentile elevation	**−0.70**	−0.17
50th percentile elevation	**−0.85**	−0.08
75th percentile elevation	**−0.95**	−0.14
Patch metrics (resistance and resilience)		
Aggregation index	**0.80**	0.15
Contagion	0.64	−0.65
Interjuxtaposition	−0.66	0.33
Large patch index	0.63	−0.02
Landscape shape index	−0.60	−0.59
Perimeter-area fractal dimension	−0.62	−0.15
Mean shape index	0.65	−0.44
Patch diversity	**−0.81**	−0.04
Gradient surface metrics (resilience)		
Skewness of point elevations	0.04	**−0.77**
Kurtosis of point elevations	0.39	**−0.74**
Directional spatial autocorrelation of elevation	0.14	−0.38
Plot size	0.06	**−0.78**

Notes: Bold values indicate statistical significance ($p < 0.05$).

methodological preferences more than any lack of awareness about the range of geomorphic and ecological processes at play. Our results, however, indicated that the sampled islands of these two regions have differing but overlapping topographies. Their topographies plotted in distinct but adjacent positions in state space, implying that these two biogeomorphic models might emphasize different levels of resistance and resilience.

Topographic Differences

As hypothesized, only two dimensions were needed to define the state space of the Virginia islands. Elevation was the overriding influence on topography. Other dune metrics had a weaker influence on topography and exhibited greater multicollinearity. This confirms that topography across all scales appears to be more coupled to exogenous geomorphic disturbances like overwash. In contrast, the Georgia Bight state space had three dimensions and less multicollinearity. As hypothesized, spatial structuring was better developed. Patch and gradient metrics loaded more robustly on higher dimensional axes and were less collinear with elevation. This points toward a greater role for endogenous biogeomorphic development. Topography is certainly subject to storm inputs in the Georgia Bight, but because the islands sampled there are not as low and erosional as the Virginia coast, dune vegetation might contribute more to landscape structure. Dune vegetation in Virginia might be more limited to anchoring functions, with less propensity for biogeomorphic feedbacks to become entrained into topography at landscape extents.

The combined state space corroborated that the topographies of the two regions were distinct but overlapping. Virginia island sites occupied a mostly separate area from those of the Georgia Bight. Based on the first axis of state space, Virginia dunes are lower and vary less in elevation over a given distance. Dune landforms are more curvilinear. The Georgia Bight topographies exhibited more rectilinear shore-parallel landforms. Topography is higher and more variable over shorter distances. The second axis of combined state space distinguished island sites based on the kurtosis, plot size, and variability in elevation within a site. The Georgia Bight islands were distributed along a longer length of the second axis than the Virginia islands, confirming that they are more strongly structured by these higher dimension resilience metrics. Dune topography tracked with island morphology along the second axis and mostly for islands in the Georgia Bight.

The separation of the Virginia barrier islands in state space is likely a consequence of their higher rates of sea-level rise and erosion. Their size and morphology might also play a role. Most of the Virginia barrier islands are tidally dominated morphologies. They are also smaller than their tidally dominated counterparts in Georgia and South Carolina. Because inlets at either end of tidally dominated islands are sources and sinks for sediments that shape adjacent shorelines, the smaller, rapidly eroding barrier islands of Virginia might have greater variability in alongshore depositional and erosional conditions (Haluska 2017) and thus distinctive topographies. Mulhern, Johnson, and Martin (2017) observed that tidally-dominated island morphologies exhibit more variability in shape than wave-dominated morphologies, a finding that can be extended to their dunes.

The distinctiveness of the Virginia islands could also be a consequence of the impacts of Hurricane Sandy in 2012. The two independent samplings of

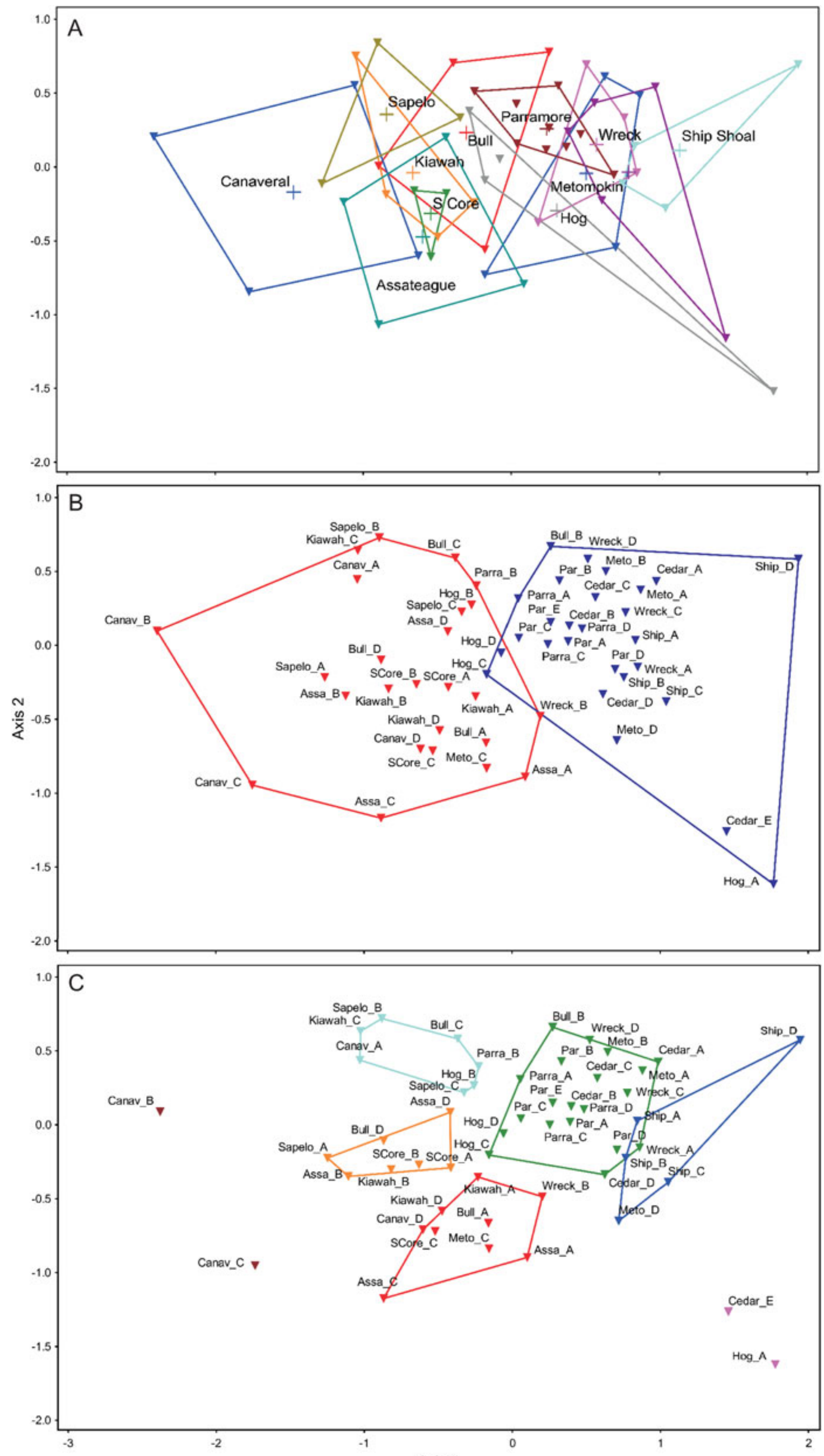

Figure 5. Nonmetric multidimensional scaling topographic state space for the combined data set: (A) island centroids, (B) two-cluster solution, and (C) seven-cluster solution. Parramore sites sampled in Monge and Stallins (2016) are abbreviated "Parra." Parramore sites sampled for this study are abbreviated "Par." Line and symbol colors indicate island membership.

Parramore Island, however, each with different LiDAR data sets (2012 and 2014), produced topographies that fell near each other in the combined state space (Figure 5B–5C). Either the topographic effects of Sandy persisted over the two years between LiDAR flights or the effects were not so much out of the ordinary for the Virginia coast. Hapke et al. (2016) found that the response to Sandy at Fire Island, New York, was not notable or distinguishable from several other large storms of the prior decade.

Table 4. Pearson's correlation coefficients for plot of nonmetric multidimensional scaling axis coordinates and topographic metrics for the combined data set

	Axis 1	Axis 2
Descriptive statistics (resistance)		
Mean elevation	**−0.89**	−0.27
Max elevation	−0.67	−0.58
25th percentile elevation	**−0.70**	−0.40
50th percentile elevation	**−0.86**	−0.19
75th percentile elevation	**−0.92**	−0.14
Patch metrics (resistance and resilience)		
Aggregation index	**0.87**	0.07
Contagion	**0.80**	−0.50
Interjuxtaposition	**−0.71**	0.37
Large patch index	**0.73**	0.10
Landscape shape index	−0.49	**−0.70**
Perimeter-area fractal dimension	−0.68	−0.16
Mean shape index	**0.78**	−0.25
Simpson's index for patch diversity	**−0.85**	−0.01
Gradient surface metrics (resilience)		
Skewness of point elevations	0.15	−0.54
Kurtosis of point elevations	0.40	**−0.72**
Directional spatial autocorrelation of elevation	0.12	−0.61
Plot size	0.32	**−0.74**

Notes: Bold values indicate statistical significance ($p < 0.05$).

Differences in Resistance, Resilience, and Biogeomorphic Models

Because of its dominant association with elevation, we posit that the first axis of the state space derived in this study represents resistance associated with the low and high island states of Vinent and Moore (2015). As originally based on dune topographies in Virginia, these high and low states relate to whether a barrier coast can maintain enough elevation through geomorphic processes and the topography-modifying capacities of dune plants to persist in a relatively high-resistance state or remain trapped in a low-resistance state subject to frequent overwash and erosion. Islands of Virginia have lower resistance than those of the Georgia Bight.

Metrics indicative of biogeomorphic resilience were correlated with the second axis of state space. Topographies along this axis spanned tidally

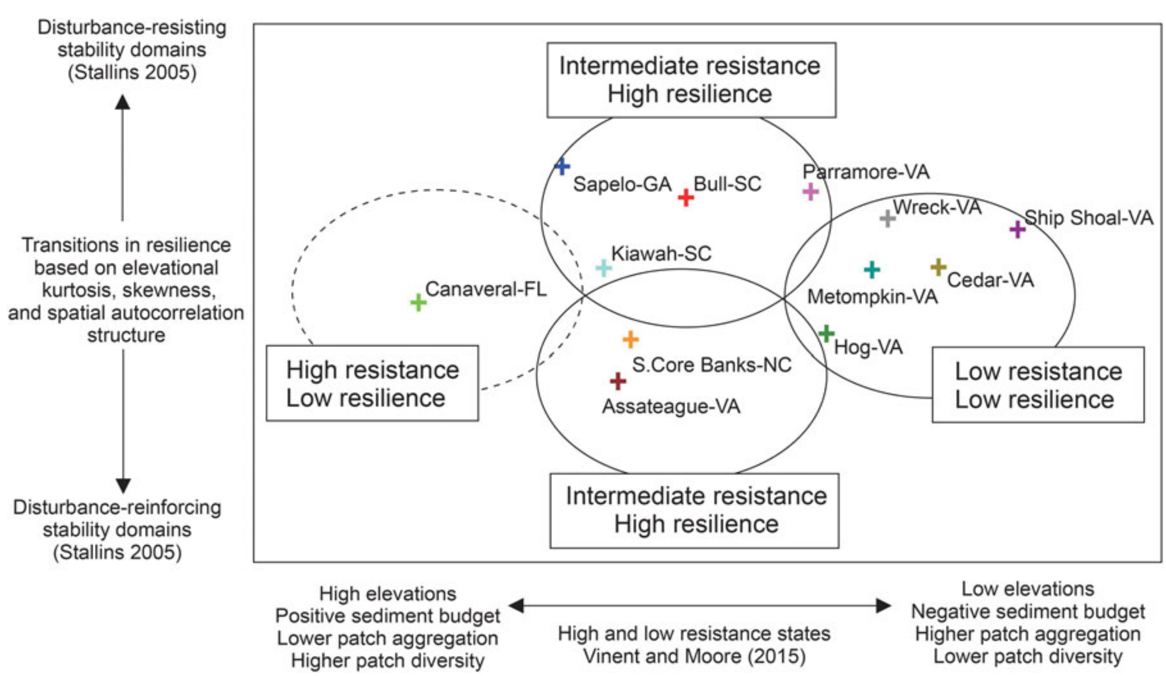

Figure 6. Summary of resilience properties in barrier island dune topographic state space. Because the Virginia coast was sampled more intensively and exerted more influence on the structure of state space, this summary also incorporates axis interpretations from the Georgia Bight state space. Intermediate elevation is approximately 1.2 ± 0.5 m relative to the high-water mark.

dominated to wave-dominated morphologies of the Georgia Bight. We suggest that this higher dimension axis captures aspects of stability domain structure affiliated with island morphology as postulated by Stallins (2005). The islands at either end of the second axis correspond to stability domain for disturbance-reinforcing islands (Assateague and South Core Banks) and disturbance-resisting islands (Sapelo, Kiawah, and Bull). Resilience might be maximized at either end of the second axis, with diminishing resilience near the middle. Based on their positions relative to the second axis, the islands of Virginia have lower resilience compared to the islands of the Georgia Bight. Resilience in Virginia is likely more limited to localized biogeomorphic feedbacks that bind and anchor sediments.

Given the smaller length of the second axis and the lower amount of variance extracted on it, resilience is likely a less frequently observed property of barrier coasts than resistance. Conditions for its development might be harder to meet. The resilience associated with island morphology developed only at intermediate elevations along the middle of this first axis. Studies from fluvial and periglacial environments specify an analogous window or envelope of conditions in which biogeomorphic resilience can emerge (Corenblit et al. 2015; Eichel, Corenblit, and Dikau 2016; Hortobágyi et al. 2018). Geomorphic disturbances might be too frequent at low elevations (Ship Shoal) or too infrequent at higher elevations (Canaveral) to allow the landscape-extent positive feedbacks among dune plant functional types, topography, and sediment mobility to evolve and generate landscape biogeomorphic resilience.

Figure 6 summarizes where islands plotted in relation to regions of resistance and resilience in state space. The first axis spans the resistance imparted by high to low elevations. It corresponds with the high and low state model of Vinent and Moore (2015). Wernette, Thompson, et al. (2018), Wernette, Houser, et al. (2018), and Houser, Wernette, and Weymer (2018) posited that changes in the scales of variability of elevation are indicative of barrier island response and recovery. The axes of state space in this study analogously summarize changes in the scale of variability in topography. Based on patch aggregation and diversity, elevation and topography change from high and variable over short distances to low and homogenous over larger areas along the first axis. The second axis spans the resilience expressed within stability domain topographies (e.g., Stallins 2005) at intermediate elevations. Transitions in skewness, kurtosis, and autocorrelation are indicative of abrupt transitions in resilience for a range of earth surface systems (Scheffer et al. 2015). The potential for these kinds of transitions was evident in this study. These three metrics were correlated with topographic changes along the second axis in the combined state space (kurtosis) and in the state space for the Georgia Bight (skewness and spatial autocorrelation). Changes in topography along the second axis might be more abrupt and threshold driven. Transitions between high and low island resistance states along the first axis might be more gradual.

Conclusions

The Virginia and Georgia Bight barrier islands occupied different regions in topographic state space. Virginia barrier islands have lower resistance and resilience. In the Georgia Bight, topographies exhibited greater resistance and resilience. Resilience was linked to wave-dominated and tidally dominated barrier island morphologies. Yet as a conditioning factor for resilience, island morphology is secondary to elevation. Intermediate elevations were necessary for resilience to be fully developed. The structure of state space conveyed how the two models invoked to describe the response and recovery of barrier dunes, those of Vinent and Moore (2015) and Stallins (2005), are complementary. They account for different levels of resistance and resilience in barrier dunes. Because each model was developed from observations in separate regions with different methods and a few simple representations of topography, it might be hasty to assume that either model has universality to the exclusion of the other.

Because of the considerable topographic variability expressed within individual islands, assuming that there is a broad geographic gradient in resistance and resilience from north to south along the southeast Atlantic coast is simplistic. Centroids were necessary to summarize the central tendencies in topography and resilience properties for the islands. Sankaran et al. (2018) argued that this kind of coarsening is required to detect resilience that has a spatial component. Spatial resilience has been shown to lack the discreteness it has in time (Génin et al. 2018). We posit that resilience might be more heterogeneously distributed along barrier dune coasts than previously assumed. Resistance is a more dominant property, perhaps as a consequence of sea-level rise underway. Phillips (2018a) also suggested that the conditions for high resilience to develop might be less dynamically favored. In this study, high resilience developed only within circumscribed regions of topographic state space.

Therefore, we caution against uncritical use of the elevation values, the sizes and shapes of landforms, and the spatial properties of dune landscapes we have inferred from state space to categorize dune topography at a specific location as resistant or resilient. Not only is resilience a spatially dynamic process but assigning resistance or resilience to topography also has to be assessed relative to the functional traits of dune vegetation, which can vary considerably in time and across space (Harris, Zinnert, and Young 2017; Goldstein et al. 2018). A plant species can have different topography-modifying functions because of its phenotypic plasticity. How it modifies topography will vary according to context. A grass species like *Spartina patens* should be expected to vary in its topography-modifying capacities from place to place (Mullins et al. 2019). Taxonomic categories like species are likely to be far less relevant than plant functional traits for understanding the vegetation component of dune topography.

The findings of this study are limited in that vegetation was not sampled, although topography and vegetation are highly interactive on coastal dunes. Although Virginia and the Georgia Bight encompass a wide range of barrier island types, we sampled only eleven islands out of the approximately 2,100 barrier islands globally (Stutz and Pilkey 2011). Adding dune topographies from Texas, the northern Gulf of Mexico, or even the German Bight are logical next steps. With more islands and repeat characterizations of topography through time, the structure of state space should converge on a solution with more predictive potential. The resilience properties inferred for regions of state space need to be assessed in terms of plant functional traits. Techniques like the power law approach of Houser, Wernette, and Weymer (2018) should also be used to verify the resilience properties of state space. Untangling the causality of biogeomorphic feedbacks and their spatial expression would give rigor to the use of the correlative associations in this study (Corenblit et al. 2019).

ORCID

J. Anthony Stallins http://orcid.org/0000-0002-3911-828X

References

Allen, C. R., D. G. Angeler, G. S. Cumming, C. Folke, D. Twidwell, D. R. Uden, and J. Bennett. 2016. Quantifying spatial resilience. *Journal of Applied Ecology* 53 (3):625–35. doi:10.1111/1365-2664.12634.

Allen, C. R., D. G. Angeler, A. S. Garmestani, L. H. Gunderson, and C. S. Holling. 2014. Panarchy: Theory and application. *Ecosystems* 17 (4):578–89. doi:10.1007/s10021-013-9744-2.

Baas, A. C. W., and J. M. Nield. 2010. Ecogeomorphic state variables and phase-space construction for quantifying the evolution of vegetated aeolian landscapes. *Earth Surface Processes and Landforms* 35 (6):717–31. doi:10.1002/esp.1990.

Brantley, S. T., S. N. Bissett, D. R. Young, C. W. Wolner, and L. J. Moore. 2014. Barrier island morphology and sediment characteristics affect the recovery of dune building grasses following storm-induced overwash. *PLoS ONE* 9 (8):e104747. doi:10.1371/journal.pone.0104747.

Collins, S. E., S. F. Matter, I. Buffam, and J. E. Flotemersch. 2018. A patchy continuum? Stream processes show varied responses to patch- and continuum-based analyses. *Ecosphere* 9 (11):e02481. doi:10.1002/ecs2.2481.

Corenblit, D., A. Baas, T. Balke, T. Bouma, F. Fromard, V. Garófano-Gómez, E. González, et al. 2015. Engineer pioneer plants respond to and affect geomorphic constraints similarly along water–terrestrial interfaces world-wide. *Global Ecology and Biogeography* 24 (12):1363–76. doi:10.1111/geb.12373.

Corenblit, D., E. Roussel, J. Steiger, and R. Walcker. 2019. A bivariate model for estimating reciprocal causality within biogeomorphic ecosystems: The cross-lagged panel model. *Earth Surface Processes and Landforms* 44 (2):667–71. doi:10.1002/esp.4535.

Corenblit, D., J. Steiger, A. M. Gurnell, E. Tabacchi, and L. Roques. 2009. Control of sediment dynamics by vegetation as a key function driving biogeomorphic succession within fluvial corridors. *Earth Surface Processes and Landforms* 34 (13):1790–1810. doi:10.1002/esp.1876.

Davidson-Arnott, R., P. Hesp, J. Ollerhead, I. Walker, B. Bauer, I. Delgado-Fernandez, and T. Smyth. 2018. Sediment budget controls on foredune height: Comparing simulation model results with field data. *Earth Surface Processes and Landforms* 43 (9):1798–1810. doi:10.1002/esp.4354.

Deaton, C. D., C. J. Hein, and M. L. Kirwan. 2017. Barrier island migration dominates ecogeomorphic

feedbacks and drives salt marsh loss along the Virginia Atlantic Coast, USA. *Geology* 45 (2):123–26. doi:10.1130/G38459.1.
Donohue, I., O. L. Petchey, J. M. Montoya, A. L. Jackson, L. McNally, M. Viana, K. Healy, M. Lurgi, N. E. O'Connor, and M. C. Emmerson. 2013. On the dimensionality of ecological stability. *Ecology Letters* 16 (4):421–29. doi:10.1111/ele.12086.
Eichel, J., D. Corenblit, and R. Dikau. 2016. Conditions for feedbacks between geomorphic and vegetation dynamics on lateral moraine slopes: A biogeomorphic feedback window. *Earth Surface Processes and Landforms* 41 (3):406–19. doi:10.1002/esp.3859.
Feagin, R., and X. B. Wu. 2007. The spatial patterns of functional groups and successional direction in a coastal dune community. *Rangeland Ecology and Management* 60 (4):417–25. doi:10.2111/1551-5028(2007)60[417:TSPOFG.2.0.CO;2]
Feagin, R., X. Wu, F. Smeins, S. Whisenant, and W. Grant. 2005. Individual versus community level processes and pattern formation in a model of sand dune plant succession. *Ecological Modelling* 183 (4):435–49. doi:10.1016/j.ecolmodel.2004.09.002.
Fonstad, M. A., and W. A. Marcus. 2010. High resolution, basin extent observations and implications for understanding river form and process. *Earth Surface Processes and Landforms* 35 (6):680–98. doi:10.1002/esp.1969.
Fuller, I. C., D. J. Gilvear, M. C. Thoms, and R. G. Death. 2019. Framing resilience for river geomorphology: Reinventing the wheel? *River Research and Applications* 35 (2):91–106. doi:10.1002/rra.3384.
Génin, A., S. Majumder, S. Sankaran, F. D. Schneider, A. Danet, M. Berdugo, V. Guttal, and S. Kéfi. 2018. Spatially heterogeneous stressors can alter the performance of indicators of regime shifts. *Ecological Indicators* 94 (1):520–33. doi:10.1016/j.ecolind.2017.10.071.
Godfrey, P. J. 1977. Climate, plant response and development of dunes on barrier beaches along the United States East Coast. *International Journal of Biometeorology* 21 (3):203–15. doi:10.1007/BF01552874.
Godfrey, P. J., S. P. Leatherman, and R. Zaremba. 1979. A geobotanical approach to classification of barrier beach systems. In *Barrier islands*, ed. S. P. Leatherman, 99–126. New York: Academic Press.
Goldstein, E. B., and L. J. Moore. 2016. Stability and bistability in a one-dimensional model of coastal foredune height. *Journal of Geophysical Research: Earth Surface* 121 (5):964–77. doi:10.1002/2015JF003783.
Goldstein, E. B., E. V. Mullins, L. J. Moore, R. G. Biel, J. K. Brown, S. D. Hacker, K. R. Jay, R. S. Mostow, P. Ruggiero, and J. C. Zinnert. 2018. Literature-based latitudinal distribution and possible range shifts of two US east coast dune grass species (*Uniola paniculata* and *Ammophila breviligulata*). *PeerJ* 6:e4932. doi:10.7717/peerj.4932.
Gutierrez, B. T., N. G. Plant, E. R. Thieler, and A. Turecek. 2015. Using a Bayesian network to predict barrier island geomorphologic characteristics. *Journal of Geophysical Research: Earth Surface* 120 (12):2452–75. doi:10.1002/2015JF003671.
Haluska, J. D. 2017. Analysis of Virginia barrier island shoreline movement and correlations to sea level, wave height changes, and teleconnection patterns. PhD diss., Old Dominion University.
Hapke, C. J., N. G. Plant, R. E. Henderson, W. C. Schwab, and T. R. Nelson. 2016. Decoupling processes and scales of shoreline morphodynamics. *Marine Geology* 381:42–53. doi:10.1016/j.margeo.2016.08.008.
Harris, A. L., J. C. Zinnert, and D. R. Young. 2017. Differential response of barrier island dune grasses to species interactions and burial. *Plant Ecology* 218 (5):609–19. doi:10.1007/s11258-017-0715-0.
Harrison, S. 2001. On reductionism and emergence in geomorphology. *Transactions of the Institute of British Geographers* 26 (3):327–39. doi:10.1111/1475-5661.00025.
Hayes, M.O. 1994. The Georgia Bight barrier system. In *Geology of Holocene barrier island systems*, ed. R. A. Davis, 233–304. Berlin: Springer.
Hillebrand, H., S. Langenheder, K. Lebret, E. Lindström, Ö. Östman, and M. Striebel. 2018. Decomposing multiple dimensions of stability in global change experiments. *Ecology Letters* 21 (1):21–30. doi:10.1111/ele.12867.
Hortobágyi, B. 2018. Multi-scale interactions between riparian vegetation and hydrogeomorphic processes (the lower Allier River). PhD diss., Université Clermont Auvergne.
Hortobágyi, B., D. Corenblit, J. Steiger, and J.-L. Peiry. 2018. Niche construction within riparian corridors. Part I: Exploring biogeomorphic feedback windows of three pioneer riparian species (Allier River, France). *Geomorphology* 305:94–111. doi:10.1016/j.geomorph.2017.08.048.
Houser, C. 2013. Alongshore variation in the morphology of coastal dunes: Implications for storm response. *Geomorphology* 199:48–61. doi:10.1016/j.geomorph.2012.10.035.
Houser, C. 2018. Barrier response to sea level rise and storms. *Earth Surface Processes and Landforms* 43 (11):2481–83. doi:10.1002/esp.4396.
Houser, C., P. Wernette, E. Rentschlar, H. Jones, B. Hammond, and S. Trimble. 2015. Post-storm beach and dune recovery: Implications for barrier island resilience. *Geomorphology* 234:54–63. doi:10.1016/j.geomorph.2014.12.044.
Houser, C., P. Wernette, and B. A. Weymer. 2018. Scale-dependent behavior of the foredune: Implications for barrier island response to storms and sea-level rise. *Geomorphology* 303:362–74. doi:10.1016/j.geomorph.2017.12.011.
Inkpen, R., and K. Hall. 2016. Using morphospaces to understand tafoni development. *Geomorphology* 261:193–99. doi:10.1016/j.geomorph.2016.03.003.
Inkpen, R., and D. Petley. 2001. Fitness spaces and their potential for visualizing change in the physical landscape. *Area* 33 (3):242–51. doi:10.1111/1475-4762.00028.
Isenburg, M. 2014. LAStools. Accessed January 6, 2018. http://www.cs.unc.edu/~isenburg/lastools.

Kedron, P. J., A. E. Frazier, G. A. Ovando-Montejo, and J. Wang. 2018. Surface metrics for landscape ecology: A comparison of landscape models across ecoregions and scales. *Landscape Ecology* 33 (9):1489–1504. doi:10.1007/s10980-018-0685-1.

Kupfer, J. A. 2012. Landscape ecology and biogeography: Rethinking landscape metrics in a post-FRAGSTATS landscape. *Progress in Physical Geography: Earth and Environment* 36 (3):400–420. doi:10.1177/0309133312439594.

Lamothe, K. A., K. M. Somers, and D. A. Jackson. 2019. Linking the ball-and-cup analogy and ordination trajectories to describe ecosystem stability, resistance, and resilience. *Ecosphere* 10 (3):e02629. doi:10.1002/ecs2.2629.

Lastochkin, A. N., A. I. Zhirov, and S. F. Boltramovich. 2018. System-morphological approach: Another look at morphology research and geomorphological mapping. *Geomorphology* 303:486–503. doi:10.1016/j.geomorph.2017.10.022.

Leatherman, S. P. 1979. *Barrier islands from the Gulf of St. Lawrence to the Gulf of Mexico*. New York: Academic Press.

Long, J., and C. Robertson. 2017. Comparing spatial patterns. *Geography Compass* 12 (2):e12356. doi:10.1111/gec3.12356.

McCune, B., and M. J. Mefford. 2016. PC-ORD. *Multivariate analysis of ecological data* (version 7). Gleneden Beach, OR: MjM Software Design.

McGarigal, K., S. A. Cushman, and E. Ene. 2012. *FRAGSTATS: Spatial pattern analysis program* (version 4.2.). Amherst: University of Massachusetts. Accessed January 6, 2019. http://www.umass.edu/landeco/research/fragstats/fragstats.html.

McGill, B. J. 2019. The what, how and why of doing macroecology. *Global Ecology and Biogeography* 28 (1):6–17. doi:10.1111/geb.12855.

Monge, J. A., and J. A. Stallins. 2016. Properties of dune topographic state space for six barrier islands of the U.S. southeastern Atlantic coast. *Physical Geography* 37 (6):452–75. doi:10.1080/02723646.2016.1230041.

Moore, L. J., and A. B. Murray. 2018. *Barrier dynamics and response to changing climate*. Cham, Switzerland: Springer.

Mulhern, J. S., C. L. Johnson, and J. M. Martin. 2017. Is barrier island morphology a function of tidal and wave regime? *Marine Geology* 387:74–84. doi:10.1016/j.margeo.2017.02.016.

Mullins, E., L. J. Moore, E. B. Goldstein, T. Jass, J. Bruno, and O. D. Vinent. 2019. Investigating dune-building feedback at the plant level: Insights from a multispecies field experiment. *Earth Surface Processes and Landforms* 44 (9). doi:10.1002/esp.4607.

Nash, K. L., C. R. Allen, D. G. Angeler, C. Barichievy, T. Eason, A. S. Garmestani, N. A. J. Graham, et al. 2014. Discontinuities, cross-scale patterns, and the organization of ecosystems. *Ecology* 95 (3):654–67. doi:10.1890/13-1315.1.

National Oceanic and Atmospheric Administration. 2012. *VDatum* (version 3.9). Accessed January 6, 2018. https://vdatum.noaa.gov/welcome.html.

Odum, W. E., T. J. Smith, and R. Dolan. 1987. Suppression of natural disturbance: Long-term ecological change on the Outer Banks of North Carolina. In *Landscape heterogeneity and disturbance*, ed. M. G. Turner, 123–35. New York: Springer.

Oertel, G. F., and J. C. Kraft. 1994. New Jersey and Delmarva barrier islands. In *Geology of Holocene barrier island systems*, ed. R. A. Davis, 207–32. Berlin: Springer.

Phillips, J. D. 2009. Landscape evolution space and the relative importance of geomorphic processes and controls. *Geomorphology* 109 (3–4):79–85. doi:10.1016/j.geomorph.2009.01.007.

Phillips, J. D. 2018a. Coastal wetlands, sea level, and the dimensions of geomorphic resilience. *Geomorphology* 305:173–84.

Phillips, J. D. 2018b. Place formation and axioms for reading the natural landscape. *Progress in Physical Geography* 42 (6):697–720.

Phillips, J. D., and C. Van Dyke. 2016. Principles of geomorphic disturbance and recovery in response to storms. *Earth Surface Processes and Landforms* 41 (7):971–79. doi:10.1002/esp.3912.

Piecuch, C. G., P. Huybers, C. C. Hay, A. C. Kemp, C. M. Little, J. X. Mitrovica, R. M. Ponte, and M. P. Tingley. 2018. Origin of spatial variation in U.S. East Coast sea-level trends during 1900–2017. *Nature* 564 (7736):400–404. doi:10.1038/s41586-018-0787-6.

Praskievicz, S. 2018. River classification as a geographic tool in the age of big data and global change. *Geographical Review* 108 (1):120–37. doi:10.1111/gere.12251.

Radchuk, V., F. Laender, J. S. Cabral, I. Boulangeat, M. Crawford, F. Bohn, J. Raedt, et al. 2019. The dimensionality of stability depends on disturbance type. *Ecology Letters* 22 (4):674–84. doi:10.1111/ele.13226.

Reiners, W. A., and K. L. Driese. 2001. The propagation of ecological influences through heterogeneous environmental space. *BioScience* 51 (11):939–50. doi:10.1641/0006-3568(2001)051[0939:TPOEIT.2.0.CO;2]

Robertson, G. P. 2008. *GS+: Geostatistics for the environmental sciences*. Plainwell, MI: Gamma Design Software.

Rogers, L. J., L. J. Moore, E. B. Goldstein, C. J. Hein, J. Lorenzo-Trueba, and A. D. Ashton. 2015. Anthropogenic controls on overwash deposition: Evidence and consequences. *Journal of Geophysical Research: Earth Surface* 120 (12):2609–24. doi:10.1002/2015JF003634.

Ryu, W., and D. J. Sherman. 2014. Foredune texture: Landscape metrics and climate. *Annals of the Association of American Geographers* 104 (5):903–21. doi:10.1080/00045608.2014.923723.

Sallenger, A. H., Jr. 2000. Storm impact scale for barrier islands. *Journal of Coastal Research* 16 (3):890–95.

Sallenger, A. H., K. S. Doran, and P. A. Howd. 2012. Hotspot of accelerated sea-level rise on the Atlantic coast of North America. *Nature Climate Change* 2 (12):884–88. doi:10.1038/nclimate1597.

Sankaran, S., S. Majumder, S. Kéfi, and V. Guttal. 2018. Implications of being discrete and spatial for detecting early warning signals of regime shifts. *Ecological*

Indicators 94:503–11. doi:10.1016/j.ecolind.2017.11.040.
Scheffer, M., S. R. Carpenter, V. Dakos, and E. H. van Nes. 2015. Generic indicators of ecological resilience: Inferring the chance of a critical transition. *Annual Review of Ecology, Evolution, and Systematics* 46 (1):145–67. doi:10.1146/annurev-ecolsys-112414-054242.
Stallins, J. A. 2005. Stability domains in barrier island dune systems. *Ecological Complexity* 2 (4):410–30. doi:10.1016/j.ecocom.2005.04.011.
Stallins, J. A. 2006. Geomorphology and ecology: Unifying themes for complex systems in biogeomorphology. *Geomorphology* 77 (3–4):207–16. doi:10.1016/j.geomorph.2006.01.005.
Stallins, J. A., and D. Corenblit. 2018. Interdependence of geomorphic and ecologic resilience properties in a geographic context. *Geomorphology* 305:76–93. doi:10.1016/j.geomorph.2017.09.012.
Stallins, J. A., J. N. Mast, and A. J. Parker. 2015. Resilience theory and Thomas Vale's plants and people: A partial consilience of ecological and geographic concepts of succession. *The Professional Geographer* 67 (1):28–40. doi:10.1080/00330124.2013.852041.
Stallins, J. A., and A. J. Parker. 2003. The influence of complex systems interactions on barrier island dune vegetation pattern and process. *Annals of the Association of American Geographers* 93 (1):13–29. doi:10.1111/1467-8306.93102.
Stutz, M. L., and O. H. Pilkey. 2011. Open-ocean barrier islands: Global influence of climatic, oceanographic, and depositional settings. *Journal of Coastal Research* 272:207–22. doi:10.2112/09-1190.1.
Sundstrom, S. M., D. G. Angeler, C. Barichievy, T. Eason, A. Garmestani, L. Gunderson, M. Knutson, et al. 2018. The distribution and role of functional abundance in cross-scale resilience. *Ecology* 99 (11):2421–32. doi:10.1002/ecy.2508.
Sundstrom, S. M., D. Angeler, A. Garmestani, J. García, and C. Allen. 2014. Transdisciplinary application of cross-scale resilience. *Sustainability* 6 (10):6925–48. doi:10.3390/su6106925.
Thoms, M. C., K. M. Meitzen, J. P. Julian, and D. R. Butler. 2018. Bio-geomorphology and resilience thinking: Common ground and challenges. *Geomorphology* 305:1–7. doi:10.1016/j.geomorph.2018.01.021.
Thoms, M. C., H. Piégay, and M. Parsons. 2018. What do you mean, "resilient geomorphic systems"? *Geomorphology* 305:8–19. doi:10.1016/j.geomorph.2017.09.003.
van Coller, A. L., K. H. Rogers, and G. L. Heritage. 2000. Riparian vegetation–environment relationships: Complimentarity of gradients versus patch hierarchy approaches. *Journal of Vegetation Science* 11 (3):337–50. doi:10.2307/3236626.
Vinent, O., and L. J. Moore. 2013. Vegetation controls on the maximum size of coastal dunes. *Proceedings of the National Academy of Sciences* 110 (43):17217–22. doi:10.1073/pnas.1307580110.
Vinent, O., and L. J. Moore. 2015. Barrier island bistability induced by biophysical interactions. *Nature Climate Change* 5 (2):158–62. doi:10.1038/nclimate2474.
Walker, I. J., R. G. D. Davidson-Arnott, B. O. Bauer, P. A. Hesp, I. Delgado-Fernandez, J. Ollerhead, and T. A. G. Smyth. 2017. Scale-dependent perspectives on the geomorphology and evolution of beach-dune systems. *Earth-Science Reviews* 171:220–53. doi:10.1016/j.earscirev.2017.04.011.
Wernette, P. A., C. Houser, B. A. Weymer, M. E. Everett, M. P. Bishop, and B. Reece. 2018. Directional dependency and coastal framework geology: Implications for barrier island resilience. *Earth Surface Dynamics* 6 (4):1139–53. doi:10.5194/esurf-6-1139-2018.
Wernette, P., S. Thompson, R. Eyler, H. Taylor, C. Taube, A. Medlin, C. Decuir, and C. Houser. 2018. Defining dunes: Evaluating how dune feature definitions affect dune interpretations from remote sensing. *Journal of Coastal Research* 346:1460–70. doi:10.2112/JCOASTRES-D-17-00082.1.
Weymer, B. A., P. Wernette, M. E. Everett, and C. Houser. 2018. Statistical modeling of the long-range dependent structure of barrier island framework geology and surface geomorphology. *Earth Surface Dynamics* 6 (2):431–50. doi:10.5194/esurf-6-431-2018.
Wolner, C. W. V., L. J. Moore, D. R. Young, S. T. Brantley, S. N. Bissett, and R. A. McBride. 2013. Ecomorphodynamic feedbacks and barrier island response to disturbance: Insights from the Virginia Barrier Islands, Mid-Atlantic Bight, USA. *Geomorphology* 199:115–28. doi:10.1016/j.geomorph.2013.03.035.
Wu, Q., F. Guo, H. Li, and J. Kang. 2017. Measuring landscape pattern in three dimensional space. *Landscape and Urban Planning* 167:49–59. doi:10.1016/j.landurbplan.2017.05.022.
Zinnert, J. C., S. T. Brantley, and D. R. Young. 2016. Bistability and the future of barrier islands. *Nature Climate Change* 6 (1):5–6. doi:10.1038/nclimate2802.
Zinnert, J. C., S. A. Shiflett, S. Via, S. Bissett, B. Dows, P. Manley, and D. R. Young. 2016. Spatial–temporal dynamics in barrier island upland vegetation: The overlooked coastal landscape. *Ecosystems* 19 (4):685–97. doi:10.1007/s10021-016-9961-6.
Zinnert, J. C., J. A. Stallins, S. T. Brantley, and D. R. Young. 2016. Crossing scales: The complexity of barrier-island processes for predicting future change. *BioScience* 67 (1):39–52. doi:10.1093/biosci/biw154.

LI-CHIH HSU is a PhD Candidate in the Department of Geography at the University of Kentucky, Lexington, KY 40506-0027. E-mail: geolchsu@gmail.com. His research interests include physical geography and geographic information systems.

J. ANTHONY STALLINS is an Associate Professor in the Department of Geography at the University of Kentucky, Lexington, KY 40506-0027. E-mail: ja.stallins@uky.edu. His research interests include the way in which geographic thought can be used as a lens to examine the ideas and practices of other sciences.